Scattering Functions of Semiflexible Polymers with and without Excluded Volume Effects

Jan Skov Pedersen*

Department of Solid State Physics, Risø National Laboratory, DK-4000 Roskilde, Denmark

Peter Schurtenberger

Institut für Polymere, ETH Zürich, CH-8092 Zürich, Switzerland

Received May 28, 1996[⊗]

ABSTRACT: Off-lattice Monte Carlo simulations on semiflexible polymer chains with and without excluded volume interactions have been performed. The model used in the simulations is a discrete representation of the worm-like chain model of Kratky and Porod applied in the pseudocontinuous limit. The ratio between the cross-section radius R of the chain and the statistical segment length b was chosen to be $R/b = 0.1$ which corresponds to the value found for polymer-like micelles. The ratio R/b is equivalent to a reduced binary cluster integral of $B = 0.30$, which is in accordance with the value for polystyrene in a good solvent. The scattering functions of the semiflexible chains have been determined with a precision of $1-2\%$ for $L/b = 0.3-640$, where L is the contour length of the chain. Numerical approximations to these functions have been determined which interpolate between the simulated functions, and these can be used in the analysis of experimental scattering data. The approximations have been used in least-squares fitting of experimental small-angle neutron scattering data from polystyrene in a good solvent.

1. Introduction

Scattering experiments on polymers and polymer-like micelles covering a broad range of scattering vectors, q, reveal a series of different regions with behaviors characteristic of the various length scales of the chains. At low q, the Guinier region associated with the overall size of the chain is observed. At slightly higher q the scattering crosses over to a power-law behavior with an exponent of -2 in Θ solvents and about $-5/3$ in good solvents. These exponents are characteristic of the (self-avoiding) random walk configuration of the chain. At higher q, one probes shorter length scales and the local stiffness of the chain shows up as a crossover to a q^{-1} behavior. At even higher q the local cross-section structure of the chains gives rise to a cross-section Guinier behavior and a strong decrease in the scattering intensity. The experimental observation of all these regions is, for most systems, only possible through the combination of static light scattering and X-ray or neutron small-angle scattering.[1−5]

Frequently the analysis of scattering data from polymers or polymer-like micelles is done in terms of asymptotic expressions which are valid in the different characteristic regions, and by considering the cross-over regions. Such analysis can only be considered to be semiquantitative, and it does not usually provide accurate results. In order to take full advantage of the information content in the data, it is desirable to perform a least-squares analysis employing a model cross section. This is important, for example, for determining the statistical segment (Kuhn) length, b, which describes the local stiffness of the chain. The Kuhn length is determined from the scattering curve around $qb = 1$; however, this region is also influenced by the power law at low q and by the cross-section Guinier region at high q.

The performance of least-squares fits to the measured data requires that analytical or numerical expressions for the scattering function are available.[5,6] Such expressions are available for semiflexible chain without excluded volume effects[6] and have also been applied in the analysis of experimental data.[7]

Polymer-like micelles are typically composed of thousands of amphiphilic molecules and are thus, for all practical considerations, continuous in nature. It can therefore be expected that the worm-like chain model of Kratky and Porod, modified to include excluded volume effects, can provide a good description of the micelles. For conventional polymers, the discrete atomic structure and the bonding configurations play important roles in determining the polymer chain configurations. However, due to the low scattering intensity at high scattering vectors, it is usually not possible to observe the local atomic structure and it is therefore not necessary to apply a model with such fine resolution. In addition, most polymers have several monomers per statistical segment length, b, and thus the worm-like chain model provides a sufficiently accurate description on length scales beyond b. However, the actual value of the statistical segment length is of course determined by the local molecular structure.[8]

Numerous studies of scattering functions for semiflexible (persistence) chains[9] *without excluded volume effect* can be found in the literature. Heine, Kratky and Roppert[10] performed Monte Carlo simulations on the discrete representation of the Kratky−Porod model[9] which has fixed valence angles and free rotation around the bonds. Simulations were done for two values of the valence angle. Similar studies were performed by Kirste,[11] who also considered chains with persistence of curvature. Sharp and Bloomfield[12] calculated the scattering function for semi-flexible chains valid for scattering vectors up to $qb < 3.1$ and for contour length $L > 10b$ using the Daniels approximation.[13,17] The same calculation was done by Burchard and Kajiwara,[14] who also performed calculations for a discrete chain with fixed valence angle using the Daniels approximation. In addition, they suggested an extrapolation procedure for obtaining the scattering function for arbitrarily large scattering vectors. However, our comparisons with more accurate determinations[6] and with the Monte

[⊗] Abstract published in *Advance ACS Abstracts,* October 1, 1996.

Carlo results described in the present paper have shown rather large discrepancies for these expressions around $qb = 3.5$. Koyama[15] has used a different approach and obtained an approximate expression for the scattering function, which involves an integral which can only be calculated numerically. Our comparisons with ref 6 and the Monte Carlo results show that the scattering functions agree for $qb \ll 1$ and $qb \gg 1$, but have large discrepancies for intermediate q values ($qb \approx 1$).

An exact calculation for infinitely long chains has been done by des Cloizeaux,[16] whereas Yamakawa and Fujii[17] have determined the scattering functions by numerical methods for $L = 0.5 - 15b$ and for $qb < 15$ using a Hermitian polynomial expansion. The scattering functions of Yamakawa and Fujii were given in tables and therefore only for discrete values of L and q. This work was extended by Yoshizaki and Yamakawa[6] also using numerical methods. Results were obtained for chains with and without persistence of curvature, and the results were parametrized in the range $qb < 10$ employing an empirical procedure. As mentioned previously, these can be used in model fitting of experimental data. However, we have found some irregular behavior of the expressions for chains without persistence of curvature for L/b around one in the region of qb values close to 10. Finally, Ragnetti and Oberthür[5] have given expressions for semi-flexible chains obtained by combining the results by Sharp and Bloomfield[12] and by des Cloizeaux.[16] However, the actual expressions given in their paper contain several errors and give functions which are discontinuous, for example, at $qb = 9.4$. With a trivial correction of the prefactor of eq 15 in their article,[5] which should be multiplied by the mass M, one obtains continuous functions up to $qb = 9.4$. As the results are based on the Sharp and Bloomfield scattering function, they can only be expected to be valid for $L > 10b$. However, one finds for $qb > 5$ relative large deviations between the scattering functions obtained by these expressions and those calculated by the numerical expressions given by Yoshizaki and Yamakawa[6] as well as with those determined by Monte Carlo simulations in the present work.

Excluded volume effects were not considered in any of the studies described in the previous paragraph, and to our knowledge very few studies of scattering functions of semi-flexible chains *with excluded volume effects* have been done. The only analytical study to our knowledge is the one by Sharp and Bloomfield.[12] The calculations were based on the Daniels approximation modified to include excluded volume effects. However, the present work has shown that the expression for the radius of gyration is not valid. Due to the approximation used, one must expect, as for the calculations without excluded volume effects, that the range of parameters (q and L/b) for which the expressions can be used is limited.

Some approximate expressions are available for flexible chains with excluded volume interactions.[18−21] The most general ones are those of Utiyama, Tsunashima, and Kurata,[21] which are based on the distribution functions for the end-to-end distance obtained from lattice Monte Carlo simulations and from direct enumeration studies.[22,23] In the calculation of the structure factor, the same distribution function is used for all inter-point distances, and this allows the scattering function to be obtained as series expansions. However, more recent Monte Carlo simulations[24,25] and renormalization group calculations[26] have shown that the

distribution functions and the expansions factors depend on the actual position of the points on the chain contour. The scattering functions determined by Utiyama et al. can give an approximate description of chains with excluded volume effects if effective parameters for the distributions and the expansions are determined.[25] However, the scattering functions can at best be valid for $qb < 1$, as the local stiffness of the chain is neglected. Furthermore, the exponents and the influence of excluded volume effects on the radius of gyration have to be determined by other methods.

Reed and Reed[27] have carried out Monte Carlo simulations on the rotational isomeric state model and have determined the scattering function of semi-flexible chains with excluded volume effects. Unfortunately, the functions were not given in a form which can be used for analysis of scattering data. In a very recent Monte Carlo study, Destrée, Lyulin, and Ryckaert[28] have determined scattering functions for a model which describes polyethylene in good and Θ conditions. Scattering functions have only been obtained for $L/b = 86$ in a good solvent and $L/b = 346$ in a Θ solvent, and these functions display the expected exponent for power-law regions as well as the expected cross-over to the $1/q$ behavior at large q.

In the present paper we describe the results of a Monte Carlo simulation study of semiflexible chains with and without excluded volume effects. The primary goal has been to obtain results with excluded volume effects and to parametrize them in such a way that they can be used for model fitting of experimental scattering data on polymer-like micelles. Static light scattering experiments have shown that excluded volume effects are important in such systems.[29] The statistical segment length of the micelles is typically 300 Å, and the cross-section radius is typically 30 Å. We have therefore used a fixed ratio of $R/b = 0.1$ in the present study. Due to the inconsistency of existing scattering functions for chains without excluded volume effects, as mentioned above, simulations have also been carried out for chains without excluded volume effects. The results have been parametrized using various methods. The most accurate (and general) method used is the one by Yoshizaki and Yamakawa.[6] In addition, we have used a new and simpler method based on power-law continuations, and we have parametrized the results for chains without excluded volume effects using a method based on the approach suggested by Burchard and Kajiwara.[14]

The derived approximations have been used for least-squares fitting of experimental small-angle neutron scattering data from polystyrene (PS) in a good solvent.[30] The expressions for chains with excluded volume effects fit the experimental data very well, and various results for the structure of the chains have been obtained. The good agreement with the scattering data for PS cooperates with the results of the analysis in ref 25 of the expansion factors determined by the Monte Carlo simulations on the model with $R/b = 0.1$. In this analysis, it was found that $R/b = 0.1$ corresponds to a reduced binary cluster integral of $B = 0.3$, which is similar to the value found for polystyrene[31,32] in good solvents.

2. Monte Carlo Simulations

The model and the procedure for Monte Carlo simulations have been described previously by Pedersen, Laso, and Schurtenberger.[25] The model is a discrete representation of the worm-like chain model of Kratky and

Porod.[9,4] The parameters of a chain are L, the contour length, and b, the statistical segment length which is a measure of the flexibility of the chain. In practice, the chain is represented by N points along the contour, so that $L = Nl_0$, where l_0 is the point separation. The statistical segment length is given by $b = l_0(1 + \cos \theta)/(1 - \cos \theta)$, where θ is the valence angle. The continuous chain is obtained by letting $N \to \infty$, $l_0 \to 0$, and $\theta \to 0$ in such a way that L/b is constant.

For the excluded volume effects the finite cross-section radius of the micelle was taken into account by placing hard spheres of radius $R = 0.1b$ at each point along the chain. Check for sphere overlap was done for points separated by more than $b/3$ along the contour, which is reasonable for $R/b = 0.1$.[25] Our previous study of the model[25] has shown that at least 1000 points on the chain are required in order to reduce the effects of finite N to less than 0.3% for the ensemble averages of the radius of gyration, R_g, and of the end-to-end distance, D_{ee}.

Monte Carlo simulations were performed by the methods described by Stellman and Gans.[33] The method uses pivot moves and a coordinate correction algorithm. The zippering method described by Stellman, Froimowitz, and Gans[34] was used for checking for chain overlap. The aim was to obtain scattering functions with an accuracy of about 1% in the range up to $qb = 10$. This requires that the influence of finite N is reduced below this value. Our simulations showed that this was obtained for chains with more than 32 points per segment length b.

Simulations were performed for chains with contour lengths of $L/b = 0.3, 0.6, 1.25, 2.5, 5, 10, 20, 40, 80, 160, 320,$ and 640. The simulations were started by generating a random (but biased) self-avoiding chain. For each length the run started with a certain number of MC steps for equilibrating the chain. The number of attempted MC steps before sampling were chosen equal to the number of points on the chain. For the calculation of the scattering function $S(q)$ stroboscopic sampling was used. The total number of generated samples were 50 000, and sampling was done for each 50 samples giving a total of 1000 samples. This does not give completely independent samples. The accuracy of $S(q)$ was estimated to be better than 1−2% for $L/b \leq 160$ and 2−3% for $L/b = 320$ and 640.

The scattering function is given by:

$$S(q) = \frac{1}{N^2}\sum_{i,j}\frac{\sin qr_{ij}}{qr_{ij}} \tag{1}$$

where N is the number of points on the chain and r_{ij} is the distance between the points with indices i and j. In order to speed up the calculation, a histogram $p(r_i)$ of distances was calculated[11] so that the scattering function could be obtained as

$$S(q) = \sum_i p(r_i)\frac{\sin qr_i}{qr_i} \tag{2}$$

with a proper normalization of $p(r)$ (to give $S(q = 0) = 1$).

After the simulations, the scattering functions were calculated in the range from $qb = 0.001$ to $qb = 20$. Only the range up to $qb = 10$ was used for the numerical parametrization. The scattering functions with excluded volume effects (see Figure 1) behave qualitatively similar to those of chains without excluded volume
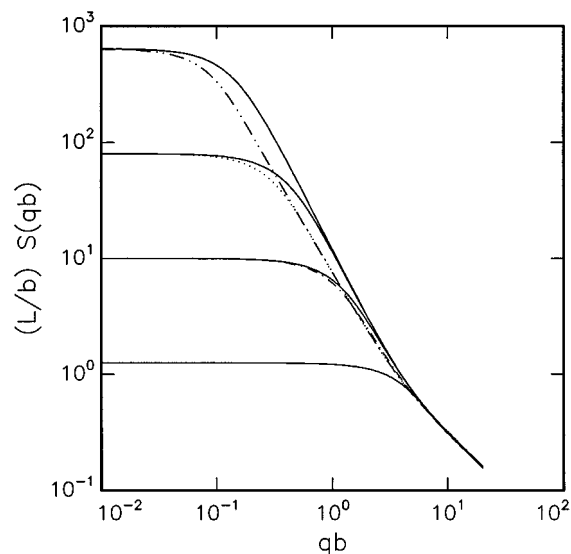

Figure 1. Scattering functions for semiflexible polymer chains in a double logarithmic representation. Monte Carlo simulations results for chains without excluded volume effects (full curve) and for chains with excluded volume effects (broken, dotted, and dashed-dotted curves). From bottom to top $L/b = 1.25, 10, 80,$ and 640, respectively.

effects.[6,9] At low q values the scattering exhibits a Guinier-type behavior. For longer chains an intermediate power-law behavior is observed with $q \propto q^{-1/\nu}$, where $\nu = 1/2$ for chains without excluded volume and $\nu = (1 + \epsilon)/2 = (1 + 0.176)/2 = 0.588$ for chains with excluded volume. At short length scales the local stiffness of the chain influences the chain conformation, and it behaves more like a stiff rod. At large q where the local structure of the chain is observed, one therefore finds a q^{-1} behavior as for rods.

3. Numerical Approximations

3.1. Method 1. Without Excluded Volume Effects. The approach for the numerical parametrization described in this section is similar to the one described by Yoshizaki and Yamakawa.[6] It is empirical and to a certain extent general, but also rather involved. The scattering function is approximated by that of a Gaussian chain at low q which crosses over, quite abruptly, to that of a rod at higher q. The crossover region is corrected by a linear combination of functions which depend on the relative contour length L/b.

We thus obtain the following expression for the scattering function:

$$S_{wc}(q,L,b) = [(1 - \chi(q,L,b))S_{chain}(q,L,b) + \chi(q,L,b)S_{rod}(q,L)]\Gamma(q,L,b) \tag{3}$$

where $S_{chain}(q,L,b)$ is the scattering function of a flexible chain without excluded volume effects and $S_{rod}(q,L)$ is the scattering function of a rod. Furthermore, $\chi(q,L,b)$ is a crossover function, and the function $\Gamma(q,L,b)$ corrects the crossover region.

The function $S_{chain}(q,L,b)$ is given by the Debye function:[35]

$$S_{Debye}(q,L,b) = 2[\exp(-u) + u - 1]/u^2 \tag{4}$$

with $u = \langle R_g^2\rangle_0 q^2$, where $\langle R_g^2\rangle_0$ is the ensemble average of the square of the radius of gyration. It is given by[36]

$$\langle R_g^2\rangle_0 = \frac{Lb}{6}\left[1 - \frac{3}{2n_b} + \frac{3}{2n_b^2} - \frac{3}{4n_b^3}[1 - \exp(-2n_b)]\right]$$
(5)

where $n_b = L/b$ is the number of statistical segments of the chain.

The function $S_{\text{rod}}(q,L)$ in (3) is the scattering function of an infinitely thin rod:[37]

$$S_{\text{rod}}(q,L) = 2\text{Si}(qL)/(qL) - 4\sin^2(qL/2)/(q^2L^2)$$
(6)

where

$$\text{Si}(x) = \int_0^x t^{-1}\sin t\, dt$$
(7)

Explicit expressions for $\chi(q,L,b)$ and $\Gamma(q,L,b)$ are given in eqs 19−23 in the paper of Yoshizaki and Yamakawa[6] (ν in eq 22 in ref 6 is zero). For completeness they will also be given here with the notation and modifications used in the present work. We have:

$$\chi(q,L,b) = \exp(-\xi^{-5})$$
(8)

The parameter ξ is given by

$$\xi = q\frac{\pi}{2L}\langle R_g^2\rangle_0$$
(9)

where $\langle R_g^2\rangle_0$ is given by (5).

The function $\Gamma(q,L,b)$ is given by:

$$\Gamma(q,L,b) = 1 + (1-\chi)\sum_{i=2}^{5}A_i\xi^i + \chi\sum_{i=0}^{2}B_i\xi^{-i}$$
(10)

where

$$A_i = \sum_{i=0}^{2}a_1(i,j)(L/b)^{-j}\exp(-10b/L) +$$

$$\sum_{i=1}^{2}a_2(i,j)(L/b)^j\exp(-2L/b)$$
(11)

and

$$B_i = \sum_{i=0}^{2}b_1(i,j)(L/b)^{-j} + \sum_{i=1}^{2}b_2(i,j)(L/b)^j\exp(-2L/b)$$
(12)

where $a_1(i,j)$, $a_2(i,j)$ $b_1(i,j)$, and $b_2(i,j)$ are coefficients independent of L and b. There are in total 35 coefficients in the parametrization (eqs 11 and 12).

The 35 parameters in the numerical parametrization were obtained by a weighted least-squares optimization. The errors on the $S(q)$ functions were set to 1%. For the chains without excluded volume effects the root-mean-square (RMS) deviation of the final fit was 0.91% and the maximum deviation between the simulated scattering functions and the numerical expressions was 2.7%. The larger discrepancies for the longest chains are probably due to the lower accuracy of the simulations for this length. The final parameters are given in Table 1.

Figure 2 show the simulated and fitted scattering functions. The good agreement is required in order to make it possible to determine the Kuhn length b from scattering data by least-squares fits. The agreement between the parametrizations and the Monte Carlo results is best displayed by residual plots. Figure 3(a)
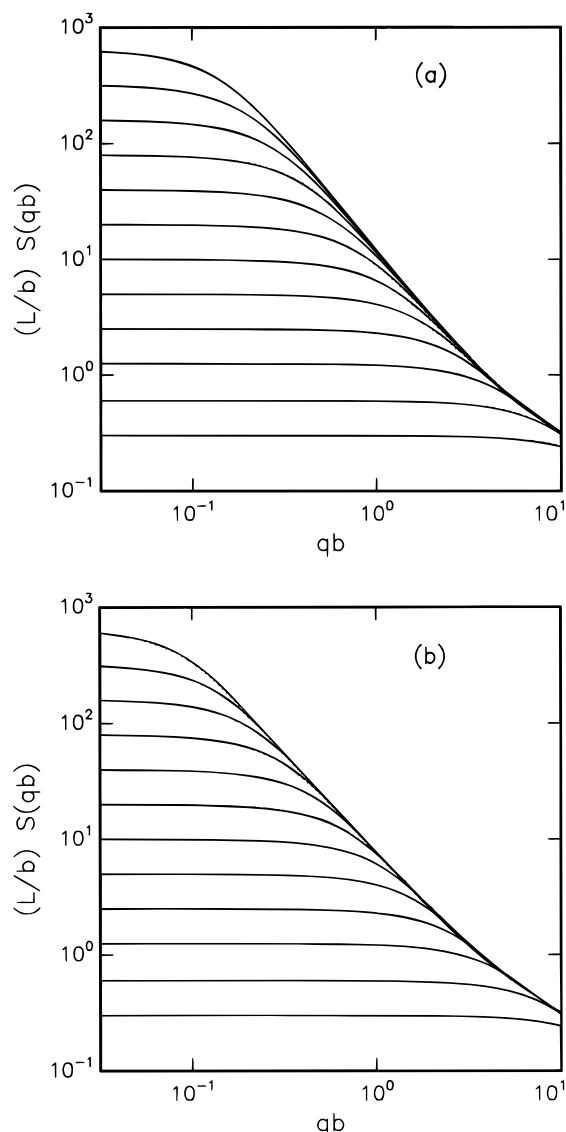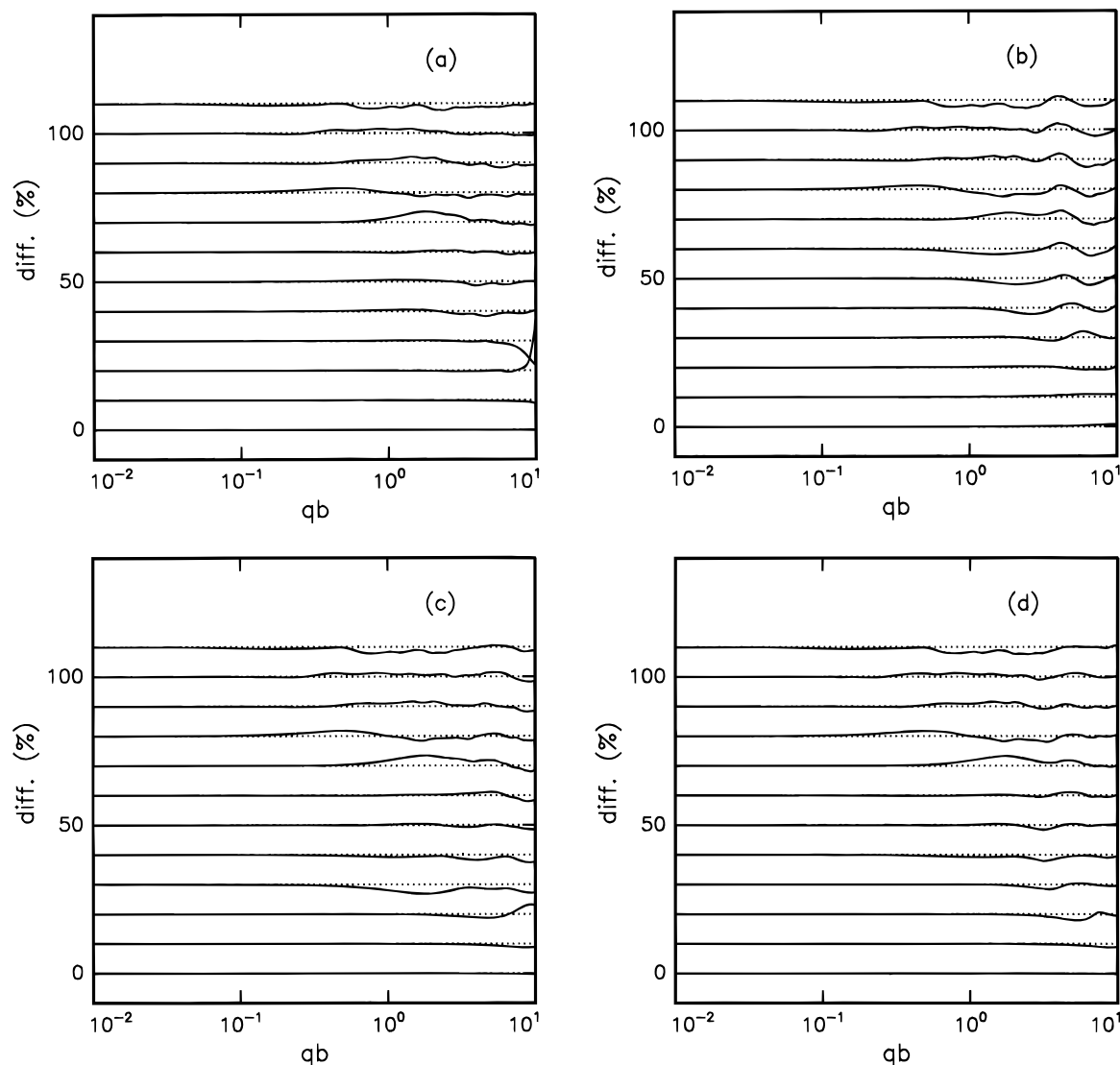

Figure 2. Scattering functions for semiflexible polymer chains in a double logarithmic representation. The dotted curves are from Monte Carlo simulations, and the full curves are the numerical approximations. The simulation data and the fits are almost indistinguishable. The curves from bottom to top are for $L/b = 0.3$, 0.6, 1.25, 2.5, 5, 10, 20, 40, 80, 160, 320, and 640, respectively. (a) Chains without excluded volume effects and (b) chains with excluded volume effects. The normalization $L/bS(qb = 0)$ is used.

shows the residual for the original parametrization of Yoshizaki and Yamakawa.[6] Large deviations are seen for $L \approx b$ around $qb = 10$. The residuals for the present parametrization are shown in Figure 3(b). They are in general of similar size as those of the original parametrization; however, the maximum deviations are considerably smaller for the present parametrization.

With Excluded Volume Effects. In Figure 1 one sees large differences between the scattering curves with and without excluded volume effects, in particular for the relatively long chains. The deviations are seen mainly at low q but also in the crossover region close to $qb = 1$. Therefore, several modifications are required in order to parametrize the scattering functions with excluded volume effects. In particular, one has to determine a scattering function for replacing the Debye function (eq 4) for a Gaussian chain, and one has to determine the appropriate values of the parameters in eqs 11 and 12.

Table 1. Values for the Parameters in the Numerical Expressions for the Scattering Function for Worm-like Chains without Excluded Volume Effects Using an Approach Similar to That of Yoshizaki and Yamakawa[6]

$a_1(2,0)$	0.3054	$a_2(2,1)$	−0.4963	$b_1(0,0)$	−0.0162	$b_2(0,1)$	−0.3946
$a_1(3,0)$	0.05777	$a_2(3,1)$	0.03688	$b_1(1,0)$	0.09046	$b_2(1,1)$	−0.2231
$a_1(4,0)$	−0.00604	$a_2(4,1)$	0.30570	$b_1(2,0)$	0.1213	$b_2(2,1)$	−0.2546
$a_1(5,0)$	−0.03902	$a_2(5,1)$	0.39013	$b_1(0,1)$	−0.3565	$b_2(0,2)$	1.1361
$a_1(2,1)$	0.2316	$a_2(2,2)$	−0.4678	$b_1(1,1)$	0.1909	$b_2(1,2)$	−0.01615
$a_1(3,1)$	2.6531	$a_2(3,2)$	0.3365	$b_1(2,1)$	0.15634	$b_2(2,2)$	−0.07606
$a_1(4,1)$	0.3706	$a_2(4,2)$	0.4290	$b_1(0,2)$	−0.3078		
$a_1(5,1)$	−1.0081	$a_2(5,2)$	0.3737	$b_1(1,2)$	0.05176		
$a_1(2,2)$	−22.779			$b_1(2,2)$	0.01568		
$a_1(3,2)$	23.2457						
$a_1(4,2)$	8.1092						
$a_1(5,2)$	−3.3603						

Figure 3. Residual plots for the parametrization for the chains without excluded volume effects. The curves from bottom to top are for L/b = 0.3, 0.6, 1.25, 2.5, 5, 10, 20, 40, 80, 160, 320, and 640, respectively. The curves are displaced by 0%, 10%, 20%, ..., 100%, and 110%, respectively. (a) The original parametrization of Yoshizaki and Yamakawa[6] (method 1). (b) The present parametrization using method 1. (c) Method 2. (d) Method 3: continuous extrapolations.

The function $S_{chain}(q,L,b)$ with excluded volume statistics was determined by fitting the expressions given by Utiyama et al.[21] to the low-q part ($qb < 1$) of the scattering functions for the longest chains determined by Monte Carlo simulations. The functions of Utiyama et al. depend on the two parameters t and s which enter the distribution function for the inter-point distances. The parameter $t = 1/(1 − \nu) = 2/(1 − \epsilon)$ (see ref 38) was fixed at $t = 2.410$ as calculated for the effective exponent $\epsilon = 0.170$ in the large-L/b limit.[25] By least-squares fit an average value of $s = 2.90$ was

determined. We note that this in only an effective value due to the nonuniform expansion of the chain and the dependence of s on which points on the chain are considered.[25]

The expression given for the scattering function by Utiyama et al.[21] consists of a low-q and a large-q expansion. In order to get good agreement at intermediate q, a large number of terms is included in the high-q expansion and this makes the numerical calculations rather slow. An approximate expression has therefore been constructed using:

$$S_{exv}(q) = w(qR_g)S_{Debye}(q,L,b) +$$
$$[1 - w(qR_g)][C_1(qR_g)^{-1/\nu} + C_2(qR_g)^{-2/\nu} + C_3(qR_g)^{-3/\nu}]$$
$$(13)$$

where $S_{Debye}(q,L,b)$ is given by eq 4 with $u = R_g^2 q^2$. $R_g = \langle R_g^2 \rangle^{1/2}$ is the radius of gyration with excluded volume effects, and it is given by[25]

$$\langle R_g^2 \rangle = \alpha(L/b)^2 \langle R_g^2 \rangle_0 \qquad (14)$$

where $\alpha(L/b)$ is the expansion factor which follows the following empirical expression:[25]

$$\alpha(x)^2 = [1 + (x/3.12)^2 + (x/8.67)^3]^{\epsilon/3} \qquad (15)$$

with an effective $\epsilon = 0.170$. Note that for $L/b > 10$ the expansion factor can also be described by the generally accepted value $\epsilon = 0.176$, when corrections to scaling are taken into account.[25] However, eq 10 fits the expansion factors in the full range of the simulations, $0.3 < L/b < 16\,384$,[25] and has a root-mean-square deviation of only 0.13% for $L/b > 10$ from the power-law fit with corrections to scaling. The function $w(qR_g)$ is an empirical crossover function chosen as:

$$w(x) = [1 + \tanh((x - C_4)/C_5)]/2 \qquad (16)$$

A least-squares fit gave $C_1 = 1.220$, $C_2 = 0.4288$, $C_3 = -1.651$, $C_4 = 1.523$, and $C_5 = 0.1477$.

The parameter ξ in the crossover function $\chi(q,L,b)$ (eq 8) was chosen as:

$$\xi = qb\left(\frac{\pi b}{1.103L}\right)^{3/2}[\langle R_g^2 \rangle/b^2]^{1.282} \qquad (17)$$

where $\langle R_g^2 \rangle$ is given by eq 14.

The parameters in eqs 11 and 12 of the numerical parametrization were obtained by a weighted least-squares optimization as described in the previous section. The RMS deviation of the final fit was 0.88%, and the maximum deviation between the simulated scattering functions and the numerical expressions was 2.2% for $L/b \leq 160$, 3.1% for $L/b = 320$, and 3.4% for $L/b = 640$. The larger discrepancies for the longest chains are probably again due to the lower accuracy of the simulations for this length. The final parameters are given in Table 2. The fits to the simulation data are shown in Figure 2, and the residuals are shown in Figure 4(a).

3.2. Method 2. Without Excluded Volume Effects. The method for parametrizing the scattering functions presented in the previous sections is quite involved, and the same can be said about the computer implementation of this method. We have therefore looked for alternative and simpler approaches. It is important to have numerically simple expressions, when analyzing experimental data for which polydispersity and instrumental resolution have to be taken into account (see also section 5). Part of the methods presented in the present section is based on the expressions used by Burchard and Kajiwara[14] in which the scattering function calculated by Sharp and Bloomfield[12] is used at low q. A crossover to the asymptotic scattering of a rod at high q by means of a simple empirical crossover function is used. However, it turns out that this method can only be used for chains with $L/b > 2$. We have therefore designed another approach for the

shortest chains, which is presented at the end of this section.

First, the parametrization for the longest chains is described. The scattering function calculated for the Daniels approximation[13] by Sharp and Bloomfield[12] is

$$S_{SB}(q,L,b) = S_{Debye}(q,L,b) + \left[\frac{4}{15} + \frac{7}{15u} - \left(\frac{11}{15} + \frac{7}{15u}\right)\exp(-u)\right]b/L \quad (18)$$

where $u = q^2 R_g^2$ and $R_g^2 = Lb/6$ is used in the Debye function. This scattering function agrees with the correct function for $L/b > 10$ and $qb < 3.1$ (see ref 17) to about 1%. At high q Burchard and Kajiwara[14] suggested to approximate the scattering function by:

$$S_{loc}(q,L) = \frac{1}{Lbq^2} + \frac{\pi}{Lq} \qquad (19)$$

where the subscript indicates that the equation should reproduce the local rod-like structure. It was further suggested to use the following interpolation expression:

$$S(q,L,b) = S_{SB}(q,L,b)\exp[-((qb)/q_1)^{p_1}] + S_{loc}(q,L)(1 - \exp[-((qb)/q_1)^{p_1}]) \quad (20)$$

where q_1 and p_1 are empirical constants. Our investigations have shown that this expression can be used for $L/b > 2$.

For $L/b \leq 2$, function 18 cannot be used at low q. We have therefore introduced the following expression:

$$S(q,L,b) = S_{Debye}(q,L,b)\exp[-((qb)/q_2)^{p_2}] + \left(\frac{a_1}{Lbq^2} + \frac{\pi}{Lq}\right)(1 - \exp[-((qb)/q_2)^{p_2}]) \quad (21)$$

where R_g in the Debye function is given by eq 5. The use of this expression for the radius of gyration gives the correct behavior of this function at low q. For the Sharp and Bloomfield scattering function, the local stiffness is taken into account through the second term in eq 18. It was furthermore necessary to include a dependence of the crossover point q_2 on L/b. We have used $q_2 = a_2 b/L$.
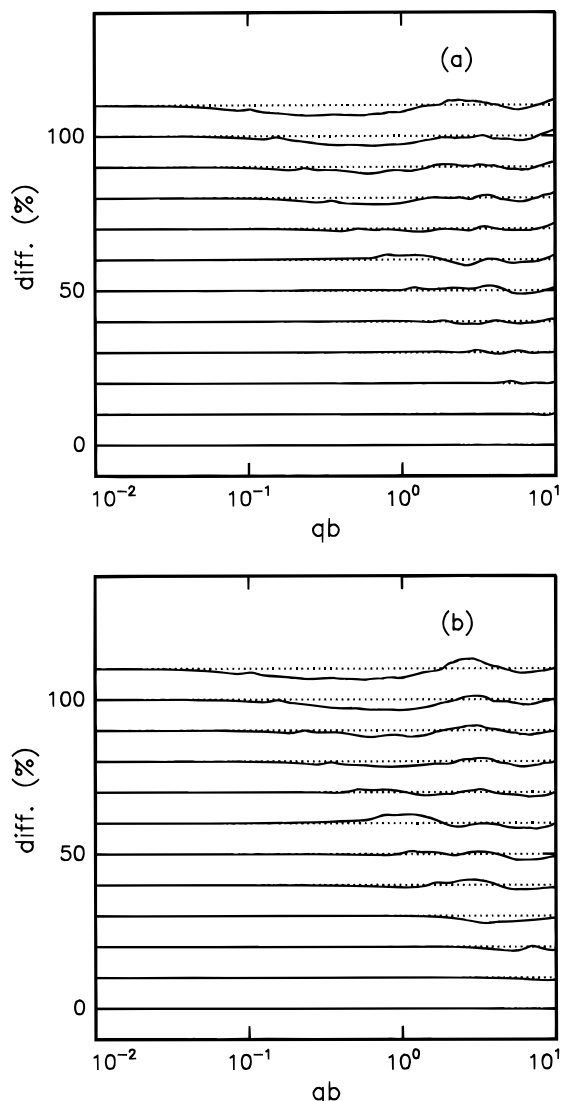
We have optimized the values of the parameters q_1, p_1, p_2, a_1, and a_2 by a least-squares fit of eqs 20 and 21 to the simulated scattering functions assuming a 1% error on the data. For $q_1 = 5.53$, $p_1 = 5.33$, $a_1 = 0.0625$, $p_2 = 3.95$, and $a_2 = 11.7$, the RMS deviation is 0.92% and the maximum deviations are 3.4% for $L = 40b$ in the range $qb < 10$. Figure 3(c) contains a plot of residuals of the parametrization.

The expressions given in this section are considerably simpler than those given by Yoshizaki and Yamakawa[6] and used in the previous section. The agreement of the expressions with the simulated scattering functions is only slightly worse. Unfortunately, we were not able to modify the equations so that they could be applied in the case of excluded volume interactions. Therefore, we implemented the method described in the next section.

3.3. Method 3. Without Excluded Volume Effects. The method presented in this section is also simpler than the method by Yoshizaki and Yamakawa (ref 6 and method 1, section 3.1). The low-q part of the scattering is described by polymer scattering functions in a similar way as done in the previous section. These functions are extrapolated by power laws which ap-

Table 2. Values for the Parameters in the Numerical Expressions for the Scattering Function for Worm-like Chains with Excluded Volume Effects Using an Approach Similar to That of Yoshizaki and Yamakawa[6]

$a_1(2,0)$	−0.1222	$a_2(2,1)$	0.1212	$b_1(0,0)$	−0.0699	$b_2(0,1)$	−0.5171
$a_1(3,0)$	0.3051	$a_2(3,1)$	−0.4169	$b_1(1,0)$	−0.0900	$b_2(1,1)$	−0.2028
$a_1(4,0)$	−0.0711	$a_2(4,1)$	0.1988	$b_1(2,0)$	0.2677	$b_2(2,1)$	−0.3112
$a_1(5,0)$	0.0584	$a_2(5,1)$	0.3435	$b_1(0,1)$	0.1342	$b_2(0,2)$	0.6950
$a_1(2,1)$	1.761	$a_2(2,2)$	0.0170	$b_1(1,1)$	0.0138	$b_2(1,2)$	−0.3238
$a_1(3,1)$	2.252	$a_2(3,2)$	−0.4731	$b_1(2,1)$	0.1898	$b_2(2,2)$	−0.5403
$a_1(4,1)$	−1.291	$a_2(4,2)$	0.1869	$b_1(0,2)$	−0.2020		
$a_1(5,1)$	0.6994	$a_2(5,2)$	0.3350	$b_1(1,2)$	−0.0114		
$a_1(2,2)$	−26.04			$b_1(2,2)$	0.0123		
$a_1(3,2)$	20.00						
$a_1(4,2)$	4.382						
$a_1(5,2)$	1.594						

Figure 4. Residual plots for the parametrization for the chains with excluded volume effects. The curves from bottom to top are for L/b = 0.3, 0.6, 1.25, 2.5, 5, 10, 20, 40, 80, 160, 320, and 640, respectively. The curves are displaced by 0%, 10%, 20%, ..., 100%, and 110%, respectively. (a) The parametrization using method 1. (b) Method 3: continuous extrapolations.

proach the scattering of a rod at high q. The extrapolation is done such that the functions and their first derivative are continuous. For the shortest chains the position of the crossover depends on the length of the chains.

For $L > 4b$ and $qb < 3.1$ we used the results of Sharp and Bloomfield[12] with $R_g{}^2 = Lb/6$. For $qb \geq 3.1$ we made the continuous extrapolation using:

$$S(q,L,b) = \frac{a_1}{(qb)^{p_1}} + \frac{a_2}{(qb)^{p_2}} + \frac{\pi}{qL} \quad (22)$$

which approaches the scattering of a rod when $qb \to \infty$. The parameters p_1 and p_2 are empirical constants, and a_1 and a_2 are determined from the requirement of continuity of $S = S(q,L,b)$ and of its first derivative $S' = dS(q,L,b)/dq$ at $qb = 3.1 = q_0$. The latter can be calculated analytically or numerically. The parameters a_1 and a_2 are given by:

$$a_2 = \left[(S + S'q_0/p_1) - \frac{\pi b}{q_0 L}(1 - 1/p_1) \right] \frac{p_1 q_0^{p_2}}{p_1 - p_2} \quad (23)$$

and

$$a_1 = Sq_0^{p_1} - a_2 q_0^{p_1 - p_2} + \frac{\pi b q_0^{p_1 - 1}}{L} \quad (24)$$

For the shorter chains the Sharp and Bloomfield expression cannot be used. We have therefore, for $L/b \leq 4$, used $S_{\text{Debye}}(q,L,b)$ with R_g given by eq 5 for $qb \leq q_0(L,b)$, where

$$q_0(L,b) = \max\{a_3 b/\langle R_g{}^2 \rangle_0^{1/2}, 4\} \quad (25)$$

For $qb > q_0(L,b)$ we used a continuous extrapolation as given by eq 22. We denote the parameters in the extrapolation for $L/b \leq 4$ by primed parameters as p'_1 and p'_2, respectively. Least-squares optimization of the parameters p_1, p_2, a_3, p'_1, and p'_2 gave a RMS deviation of 0.76% and a maximum deviation of 3.3% for $L = 40b$. The values of the optimized parameter are $p_1 = 4.95$, $p_2 = 5.29$, $p'_1 = 5.13$, $p'_2 = 7.47$, and $a_3 = 2.02$. The residuals of the parametrization are shown in Figure 3(d).

With Excluded Volume Effects. The approach used for excluded volume effects is similar to that described in the previous section. As the Sharp and Bloomfield expression is not valid for chains with excluded volume effects, it was therefore modified. We have exchanged the Debye function in expression 18 by that of a flexible chain with excluded volume effects. However, our investigations have shown that the second term in eq 18, which takes into account the local stiffness of the chains, has to be reduced by a factor which depends on L/b.

For $L > 4b$ and $qb < 3.1$ the function is:

$$S_{\text{SB}}(q,L,b) = S_{\text{exv}}(q,L,b) +$$
$$C(L/b)\left[\frac{4}{15} + \frac{7}{15u} - \left(\frac{11}{15} + \frac{7}{15u} \right) \exp(-u) \right] b/L \quad (26)$$

where $S_{\text{exv}}(q,L,b)$ is given by eq 13 with $\langle R_g{}^2 \rangle =$

$\alpha(L/b)^2 bL/6$, with $\alpha(x)$ given by eq 15. The parameter $u = \langle R_g^2 \rangle q^2 = \alpha(L/l)^2 q^2 bL/6$ and $C(L/b) = a_4/(L/b)^{p_3}$ for $L > 10b$ and $C(L/b) = 1$ for $L \leq 10b$. For $qb \geq 3.1$ we made a continuous extrapolation as done in the previous section for chains without excluded volume effects. The empirical parameters are p_1, p_2, a_4, and p_3.

For $L \leq 4b$ we do not expect the Sharp and Bloomfield type expression (eq 26) to be valid. However, for such short chains the influence of the excluded volume effects is quite small and one can therefore use an approach similar to the one described in the previous section for the short chains. We have used $S_{Debye}(q,L,b)$ with R_g given by eq 14 for $qb \leq q_0(L,b)$, where $q_0(L,b)$ is given as

$$q_0 = \max\{a_3 b/\langle R_g^2 \rangle^{1/2}, 3\} \qquad (27)$$

For $qb \geq q_0(L,b)$ we used continuous extrapolations as in the previous section involving the parameters p'_1 and p'_2 as the powers of the two power-law corrections.

The parameters were determined by a least-squares optimization as described in the previous sections. The resulting values are $p_1 = 4.12$, $p_2 = 4.42$, $a_4 = 3.06$, $p_3 = 0.44$, $a_3 = 1.9$, $p'_1 = 5.36$, and $p'_2 = 5.62$. The RMS deviation for these values is 1.05% with a maximum deviation of 3.6% for $L = 640b$ and 3.4% for $L = 320b$. The residuals are shown in Figure 4(b).

4. Examples: Polystyrene

The expressions determined in the previous section make it possible to perform a quantitative analysis of experimental scattering data for polymers in a good solvent as well as in a Θ solvent. In order to demonstrate the importance of the new results for chains with excluded volume, we have used data from the literature for polystyrene (PS) in a good solvent.

The scattering functions of atactic PS in carbon disulfide (CS$_2$) with different selective deuteration of the polymer have been determined by Rawiso, Duplessix, and Picot[30] using small-angle neutron scattering. CS$_2$ is a good solvent for PS, and this is also reflected in the scattering functions which show a $q^{-1.7}$ behavior at intermediate q values. In the original paper of Rawiso et al. the data were not fitted in the full q range as the appropriate scattering functions were not available. In the following it will be demonstrated that the parametrized scattering functions for the chains with excluded volume effects can be used for fitting the data and obtaining results for the Kuhn length b and the cross-section radii. For the shorter chains the contour length can also be determined.

The Monte Carlo simulations on the semi-flexible chain model were carried out for $R/b = 0.1$. The analysis (see ref 25) of the expansion factors for the model have shown that this corresponds to a reduced binary cluster integral of $B = 0.3$ which is similar to the value found for polystyrene[31,32] in good solvents. It can therefore be expected that the scattering functions are applicable to the scattering data for PS measured by Rawiso et al.

The polymers[30] were available with three different selective deuterations: (i) fully deuterated, (ii) deuterated in the phenyl ring, and (iii) deuterated in the backbone. CS$_2$ has a low scattering length density, and C and D have relatively large scattering length, whereas H has a negative scattering length. Therefore, it is mainly the deuterated parts of PS which contribute to the scattering.

The scattering data in Figures 2, 8(a), and 9 of the paper by Rawiso et al.[30] have been digitized. These data are for PS with molecular weights of $M_w \approx 50\,000$ and $M_w > 10^6$ corresponding to degrees of polymerization of $n \approx 500$ and $n > 10\,000$, respectively. Data sets free of concentration effects were obtained by combining the low-q data in Figures 8(a) and 9 with the high-q data in Figure 2. Note, that all the data sets are recorded for concentrations below the overlap concentration c^* and therefore the concentration effects are negligible at high q. The combined data sets are shown in Figure 5. For $M_w \approx 50\,000$ a Guinier region with a crossover to constant intensity is found at low q. The radius of gyration is $R_g \approx 85$ Å. For $M_w > 10^6$, $R_g > 540$ Å and the Guinier region falls outside the measured q range, and the power-law behavior is observed down to the smallest q values for which the scattering functions have been measured.

The data sets have been fitted by the parametrized scattering functions. The finite cross sections of the PS chains were approximated by a locally cylindrical shape using:[30,7,40,41]

$$S(q) = S_{chain}(q)\, S_{cs}(q) \qquad (28)$$

where

$$S_{cs}(q) = [2J_1(Rq)/(Rq)]^2 \qquad (29)$$

in which $J_1(x)$ is the first order Bessel function and R is the cross-section radius.

In order to reduce the number of fitting parameters, the six data sets were fitted simultaneously using the same Kuhn length for all six data sets and the same cross-section radius for the data sets with similar types of deuterations (fully/phenyl/backbone, respectively). Furthermore, the contour length for $M_w > 10^6$ was fixed at $L = 30\,000$ Å for all three data sets as it does not influence the data in the measured q range. For $M_w \approx 50\,000$ the contour lengths for the different deuterations were fitting parameters.[45] This approach was chosen due to the rather large polydispersity index of the PS ($M_w/M_n = 1.15-1.3$) as well as some expected inaccuracy of the procedure used for the extrapolation to zero concentration.[30] Additional fitting parameters were six overall scale factors and six parameters for describing residual background in the individual data sets.

The model scattering functions including excluded volume effects give almost perfect fits to the data (Figures 5(a) and -(b)). The Kuhn length is determined to $b = 24.8$ Å, in good agreement with previous determinations from small-angle scattering data ($b = 22-27$ Å) and in reasonable agreement with the value obtained from the plateau modulus of a melt ($b = 17$ Å).[39] The contour lengths of the $M_w \approx 50\,000$ polymer are $L = 1270$, $L = 1310$, and $L = 1590$ Å for the three different deuterations (i), (ii), and (iii), respectively. These are in good agreement with the values which can be calculated directly from molecular weights and the structure taking into account the polydispersity: $L_z = L_w(1 + 2U)/(1 + U)$, where L_w is the contour length for a polymer of mass M_w and $U = M_w/M_n - 1$. The values for L_z are 1360, 1360, and 1810 Å for the three deuterations, respectively.

Combining the value for the Kuhn length b with the values for the contour L, one obtains the number of statistical segments in the chains. It is $L/b \approx 50$ for $M_w \approx 50\,000$ and $L/b > 1200$ for $M_w > 10^6$. It is quite clear that the excluded volume effects are important and
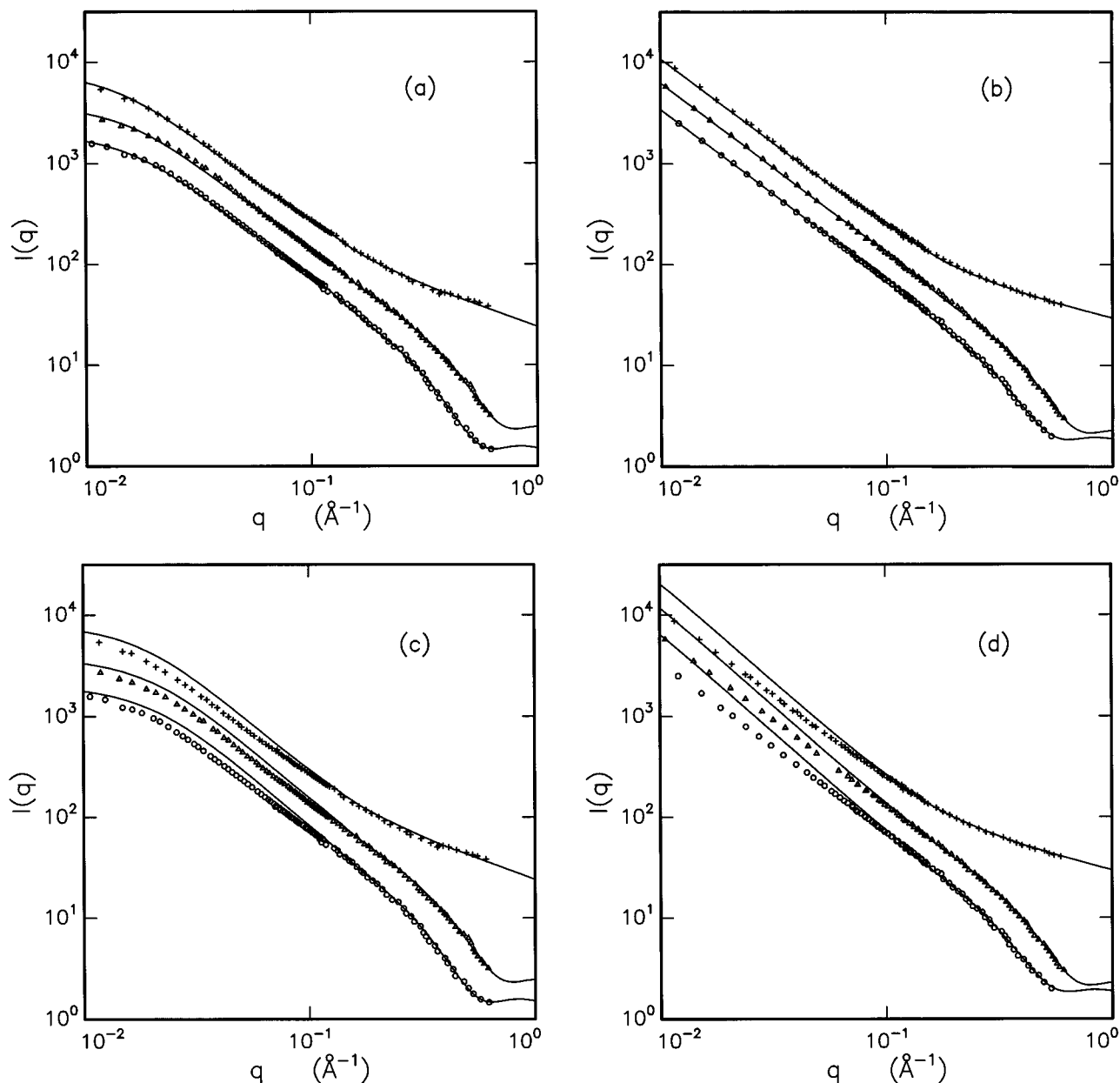
Figure 5. Scattering functions for PS in CS_2.[30] The lower data are for fully deuterated PS, the middle data are for the phenyl ring deuterated, and the upper data are for the backbone deuterated. (a) $M_w \approx 50\,000$. The curves are the fits for model scattering functions including excluded volume effects. (b) $M_w > 10^6$. The curves are the fits for model scattering functions including excluded volume effects. (c) $M_w \approx 50\,000$. The curves are for model scattering functions without excluded volume effects. (d) $M_w > 10^6$. The curves are the model scattering functions without excluded volume effects.

that they are particularly important for the chains with $M_w > 10^6$. This is also reflected in the expansion factors for R_g which are about 1.2 and 1.5, respectively.

The cross-section radii of the chains are $R = 6.0$ Å for the fully deuterated chain, $R = 4.8$ Å for the phenyl-deuterated chain, and $R < 1.0$ Å for the backbone-deuterated chain. These are quite reasonable considering the molecular structure of the PS chain. The values also agree with those determined by Rawiso et al.[30] from the high-q part of the data, and with the value $R = 8.1$ Å estimated by small-angle X-ray scattering.[4]

In Figures 5(c) and -(d) we show the scattering functions for chains without excluded volume effects with the same values for the contour length, Kuhn length, and cross-section radii. These model functions do not agree with the measured data. It is clear that excluded volume effects are very important for $q < 0.1$ Å^{-1}. In this region the experimental data display a

slope in the log−log plots which is quite different from the model functions, even for $M_w \approx 50\,000$. If the contour lengths are fixed and the data are fitted in the range $q > 0.03$ Å^{-1}, one obtains reasonable fits in this region, however, with clear systematic deviations. The fit gives a Kuhn length of 37 Å which is 50% larger than the one determined from the fit with the functions which includes excluded volume effects. This clearly shows the importance of having appropriate expressions for the scattering function of polymers with excluded volume effects, when attempting to experimentally determine an important structural parameter like the Kuhn length from the small-angle scattering data. It demonstrates that excluded volume effects not only influence the scattering data in the power-law regime, but also modify the scattering function on a much more local length scale. Therefore, one cannot use an approach in which one applies expressions valid for worm-

Table 3. Summary of the Accuracy of the Approximations in Section 3[a]

	without excluded vol		with excluded vol	
	RMS (%)	max dev (%)	RMS (%)	max dev (%)
method 1	0.91	2.7	0.88	3.4
method 2	0.92	3.4		
method 3	0.76	3.3	1.05	3.6

[a] "RMS" is root-mean-square deviation and "max dev" is the maximum deviation.

like chains without excluded volume effects at high q in order to estimate b from the crossover region around $bq = 1$. Such an approach leads to a systematic overestimation of b.

5. Discussion and Conclusions

We have performed Monte Carlo simulations on semiflexible chains with and without excluded volume effects in the pseudocontinuous limit. The scattering functions were obtained with an accuracy of $1-2\%$. The functions have been parametrized by different numerical expressions which can be used in an analysis of experimental scattering data. Method 1, following Yoshizaki and Yamakawa,[6] is the most general one and also the most accurate. However, it only gives slightly more accurate parametrizations than methods 2 and 3. This is demonstrated by the residuals shown in Figures 3 and 4. An overview of the quality of the fits is given in Table 3, which contains the root-mean-square and maximum deviations for the three parametrizations.

As a test of the applicability of the expressions for determining L and b, we have used the final expressions for analyzing the scattering functions determined by Monte Carlo simulations by means of least-squares methods. In general, it is possible to determine L and b for $L/b > 2.5$. For shorter length the scattering functions do not contain enough information for separating the two parameters. For chains without excluded volume effects, L and b can be determined with an accuracy of 1% and 2%, respectively, for all three different types of parametrizations. The RMS deviations are always less than 1%. For chains with excluded volume effects, method 1 gives b with an accuracy of about 2%, except for $L/b = 320$ and 640, where the accuracy is 3.5% and 5%, respectively. For method 3, b is accurate to about $4-5\%$. For both methods 1 and 3, L is determined with an accuracy of about 1%. The RMS deviations are less than 1% for both methods except for $L/b = 640$, where it is about 1.3% and 1.8% for methods 1 and 3, respectively. The overall conclusion from these tests is that the parametrizations can be used for determining L and b with an accuracy which in most cases is considerably better than 5%.

In an analysis of experimental data the duration of the calculation is an important issue. It is particular important for polydisperse systems[25,29] and when instrumental smearing effects have to be considered. The polydispersity is quite large for micellar equilibrium structures,[29] and it has to be included in the data analysis by convoluting the scattering function by the size distribution. For small-angle neutron scattering experiments the instrumental smearing has to be included in the data analysis, and this also involves at least one numerical integral.[42,43]

Due to the large number of terms required in the function $\Gamma(q,L,b)$, method I is relatively slow. For chains without excluded volume effects the numerical calculation in method 1 is, in our implementation, about 7

times slower than methods 2 and 3. For chains with excluded volume effects, method 1 is about $3-4$ times slower than method 3. The smaller difference in this case is due to the fact that a larger part of the time is used for calculating $S_{chain}(q,L,b) = S_{exv}(q,L,b)$.

The expressions given in the present paper in section 3 for the scattering function do not include a finite size of the cross section of the (locally) cylindrical shape. For cross-section profiles with local cylindrical symmetry this can be included as described in the previous section[30,7,40,41] by multiplying the scattering function of the chain $S(q)$ by the cross-section scattering function. In some cases the cross-section scattering length density distribution is not constant. In this case $S_{cs}(q)$ is given by the absolute square of the Hankel transform of the cross-section scattering length density profile $\Delta\rho(r)$:

$$S_{cs}(q) = |2\pi \int \Delta\rho(r) \, B_0(q,r) \, r \, dr|^2 \qquad (30)$$

where $B_0(x)$ is the zeroth order Bessel function. For analysis of scattering data from polymer-like micelles, the finite size of the cross section has to be included for accurate modeling of SANS data up to scattering vectors larger than about $0.05-0.1$ Å^{-1}.[7,40,44] In a future paper[44] we will present the results of an extensive application of the expressions for the scattering function given in the present paper. The studied systems are water-in-oil microemulsions of lecithin in cyclohexane and isooctane with trace amounts of water. The application requires the inclusion of polydispersity and instrumental smearing, as well as a two-step profile for the cross-section structure.

Examples with application to experimental data have been given in section 4. The derived approximations have been used for least-squares fitting experimental small-angle neutron scattering data from polystyrene (PS) in a good solvent.[30] Scattering functions for chains with excluded volume effects gave good fit to the data, and results for contour length, Kuhn length, and cross-section radii have been obtained. The contour lengths agree with those calculated from the molecular mass and polydispersity indices, and the determined Kuhn length of $b = 24.9$ Å is in good agreement with values found in the literature. The scattering functions for chains without excluded volume effects are not able to fit the data for PS, and even if the fitted q range is restricted to $qb > 1$, this will result in incorrect values for the Kuhn length. This demonstrates the importance of having parametrized scattering functions for chains with excluded volume effects.

The parametrized scattering functions have also been used for fitting the scattering functions for polyethylene determined by Destrée et al.[28] by Monte Carlo simulations. An excellent fit was obtained for the chain with 1025 monomers in good solvent conditions for $q < 1$ Å^{-1} using the expression for chains with excluded volume effects. The fit to the scattering function for chains with 4097 monomers in Θ conditions for $q < 1$ Å^{-1} using the expressions for chains without excluded volume effects is slightly worse. The exponent of the power law in the intermediate q range of the simulation data is higher than the model functions, which probably indicates that the simulations were done for conditions which were slightly within the poor solvent region. This is also in agreement with the fact that the radius is slightly smaller than expected at the Θ point.[28] The average Kuhn length for the two fits is $b = 14.7$ Å, in almost perfect agreement with the estimate of $b = 14.9$ Å given

by Destrée et al.[28] These examples once more show the applicability of the parametrized functions.

References and Notes

(1) Marignan, J.; Appell, J.; Basserau, P.; Porte, G.; May, R. P. *J. Phys. (Paris)* **1989**, *50*, 3553.

(2) Appell, J.; Marignan, J. *J. Phys. II* **1991**, *1*, 1447.

(3) Schurtenberger, P.; Magid, L. J.; King, S. M.; Lindner, P. *J. Phys. Chem.* **1991**, *95*, 4173.

(4) Kirste, R. G.; Oberthür, R. C. In *Small Angle X-ray Scattering*; Glatter, O., Kratky, O., Eds.; Academic Press: London, 1982.

(5) Ragnetti, M.; Oberthür, R. C. *Colloid Polymer Sci.* **1986**, *264*, 32.

(6) Yoshizaki, T.; Yamakawa, H. *Macromolecules* **1980**, *13*, 1518.

(7) Pedersen, J. S.; Egelhaaf, S. U.; Schurtenberger, P. *J. Phys. Chem.* **1995**, *99*, 1299.

(8) Yoon, D. Y.; Flory, P. J. *Macromolecules* **1976**, *9*, 294.

(9) Kratky, O.; Porod, G. *Rec. Trav. Chim. Pays-Bas* **1949**, *68*, 1105.

(10) Heine, S.; Kratky, O.; Roppert, J. *Makromol. Chem.* **1962**, *56*, 150.

(11) Kirste, R. G. In *Small-Angle X-ray Scattering* Brumberger, H., Ed.; Gordon and Breach: New York, 1967.

(12) Sharp, P.; Bloomfield, V. A. *Biopolymers* **1968**, *6*, 1201.

(13) Daniels, H. E. *Proc. R. Soc. (Edinburgh)* **1954**, *53A*, 290.

(14) Burchard, W.; Kajiwara, K. *Proc. R. Soc. London* **1970**, *A316*, 185.

(15) Koyama, R. *J. Phys. Soc. Jpn.* **1973**, *34*, 1029.

(16) des Cloizeaux, J. *Macromolecules* **1973**, *6*, 403.

(17) Yamakawa, H.; Fujii, M. *Macromolecules* **1974**, *7*, 649.

(18) Ptitsyn, O. B. *Zh. Fiz. Khim.* **1957**, *31*, 1091.

(19) Benoit, H. *C. R. Acad. Sci.* **1957**, *245*, 2244.

(20) McIntyre, D.; Mazur, J.; Wims, A. M. *J. Chem. Phys.* **1968**, *49*, 2896.

(21) Utiyama, H.; Tsunashima, Y.; Kurate, M. *J. Chem. Phys.* **1971**, *55*, 3133.

(22) Mazur, J. *J. Res. Natl. Bur. Stand.* **1965**, *A69*, 355; *J. Chem. Phys.* **1965**, *43*, 4354.

(23) Domb, C.; Gillis, J.; Wilmers, G. *Proc. Phys. Soc. (London)* **1965**, *625*, 19.

(24) Baumgärtner, A. *Z. Phys. B* **1981**, *42*, 254.

(25) Pedersen, J. S.; Laso, M.; Schurtenberger, P. Submitted to *Phys. Rev. E*, 1996.

(26) des Cloizeaux, J. *J. Phys. (Paris)* **1980**, *41*, 223.

(27) Reed, C. E.; Reed, W. F. *J. Chem. Phys.* **1992**, *97*, 7766.

(28) Destrée, M.; Lyulin, A.; Ryckaert, J.-P. *Macromolecules* **1996**, *29*, 1721.

(29) Schurtenberger, P.; Cavaco, C. *J. Phys. Chem.* **1994**, *98*, 5481.

(30) Rawiso, M.; Duplessix, R.; Picot, C. *Macromolecules* **1980**, *13*, 1518.

(31) Yamakawa, H.; Shimada, J. *J. Chem. Phys.* **1985**, *83*, 2607.

(32) Abe, F.; Einaga, Y.; Yoshizaki, T.; Yamakawa, H. *Macromolecules* **1993**, *26*, 1884.

(33) Stellman, S. D.; Gans, P. J. *Macromolecules* **1972**, *5*, 516.

(34) Stellman, G. D.; Froimowitz, M.; Gans, P. J. *J. Comput. Phys.* **1971**, *7*, 178.

(35) Debye, P. *J. Phys. Colloid Chem.* **1947**, *51*, 18.

(36) Benoit, H.; Doty, P. *J. Phys. Chem.* **1953**, *57*, 958.

(37) Neugebauer, T. *Ann. Phys. (Leipzig)* **1943**, *42*, 509.

(38) Fisher, M. E. *J. Chem. Phys.* **1966**, *44*, 616.

(39) Aharoni, S. M. *Macromolecules* **1983**, *16*, 1722.

(40) Pedersen, J. S.; Schurtenberger, P. *J. Appl. Crystallogr.* **1996** (in press).

(41) Schurtenberger, P.; Jerke, G.; Cavaco, C.; Pedersen, J. S. *Langmuir* **1996**, *12*, 2433.

(42) Pedersen, J. S.; Posselt, D.; Mortensen, K. *J. Appl. Crystallogr.* **1990**, *23*, 321.

(43) Barker, J. G.; Pedersen, J. S. *J. Appl. Crystallogr.* **1995**, *28*, 105.

(44) Jerke, G.; Schurtenberger, P.; Pedersen, J. S. To be submitted to *J. Phys. Chem.*, 1996.

(45) The molecular weight of the samples for the three different types of deuterations varies significantly. For fully/phenyl/backbone deuterated PS, the molecular weights are 53 500, 48 500, and 63 000, respectively.